

"Corrosion Performance of Laser Clad Overlays and Thermal Spray Coatings: A Comparison"

by Sunil Musali, Dr. George Kim, Peter Longobardi and Michael Breitsameter of FW Gartner, Houston Texas

Abstract

This research addresses the comparison study of corrosion characteristics of three different coating materials applied using laser cladding and thermal spraying techniques. The corrosion resistance of each coating is determined by measuring the Corrosion Penetration Rate (CPR) using three different experimental methods: (1) open circuit potential measurements, (2) potentiodynamic tests, and (3) gravimetric measurements of anodic corrosion rate.

Coating properties like surface morphology, phase analysis, structure, hardness are examined using SEM, XRD and Vickers micro hardness tester respectively. Results show that laser cladding generates superior corrosion resistant coatings in comparison to thermal spray coatings. It is evident from the results that the laser clad overlays show corrosion resistance equivalent to wrought material.

1. Introduction:

The demand for corrosion resistant coatings has been around a long time. New coating materials are constantly being developed along with new coating methods. It is generally accepted that the corrosion resistance of a coating is the result of both the material selected and method used to produce the coating. Selecting the right coating for an application often requires the balancing of process capability, cost and desired service life.

Open circuit potential vs. time for Fe 37, HVOF (High Velocity Oxygen Fuel) sprayed Inconel 625 (IN-625) coating, IN-625 laser clad coating, and wrought IN-625 alloy comparison study indicates that IN 625 laser clad coating behaves similarly with the corresponding wrought IN 625 alloy. This indicates a high corrosion resistance of the laser clad coatings [1].

Simard et al. [2] have studied comparison behavior of wrought 316 SS with HVOF sprayed 316 SS. The results demonstrated that the material behavior in regards to corrosion was process dependant. Also, HVOF sprayed 316 SS coating proved to be more sensitive to corrosion than wrought stainless steel.

Electrochemical behavior of thermal sprayed coatings indicated poor corrosion resistance [3]. Coatings containing molybdenum appeared to exhibit corrosion resistance comparable to bulk AISI 316 [3, 4].

Silitonen et al. [5] have studied the corrosion properties of stainless steel coatings produced by different thermal spray methods and found that porosity [5, 9] in the coatings and oxidation [6] of elements play a major role in impacting the corrosion

"Corrosion Performance of Laser Clad Overlays and Thermal Spray Coatings: A Comparison"

properties of coatings. They also found out that the performance of thermal spray coatings can be improved by sealing the coating with polymers.

Determination of corrosion characteristics for coatings has been traditionally done by salt spray test (ASTM G85), however new methods have been developed to keep up with improved industry standards. Magnani et al. [7] have studied the corrosion potential behavior of HVOF sprayed AA7050 Aluminum alloy using open circuit potential measurement [8, 9] which was evaluated in 3.5% NaCl [10] solution.

2. Experimental Procedure

2.1 Coating Methods

1kW (Fig 1, A) laser was used to produce laser clad coatings. The 1kW laser is direct-diode laser with an optical engine coupled to an optical fiber for transmitting the beam to the process head. The process head used for these tests was a Precitec head fitted with coaxial powder feed capabilities. The head was mounted to an eight axis robotic arm model: Fanuc Robot Arc Mate 120 with R-J2 controller for manipulation purposes. Thermach INC. model: AT 1200 powder feeder was used.

Jetkote model: JK3000(Fig1, B) High Velocity Oxygen Fuel (HVOF) system mounted to an eight axis robot model: Motoman UP 20 M with XRC 2001 controller was used to produce thermal spray coatings. Plasmadyne model: PF-50 powder feeder was used.

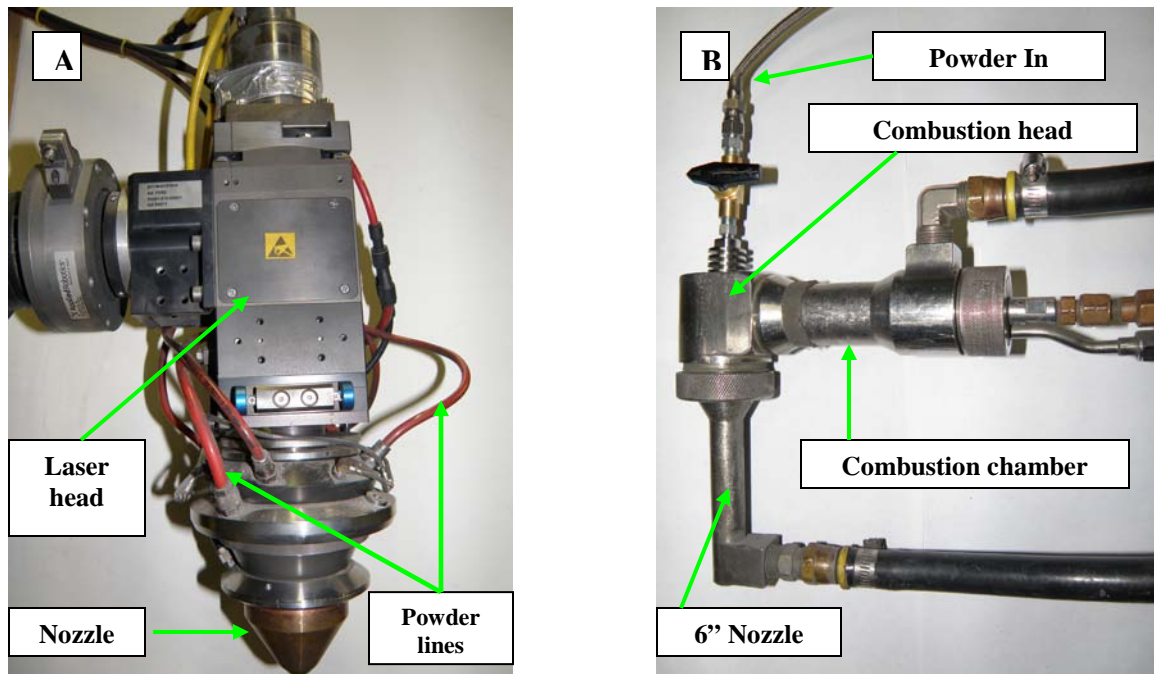


Fig. 1: (A) 1kW Laser, (B) Jet Kote 3000 HVOF gun

"Corrosion Performance of Laser Clad Overlays and Thermal Spray Coatings: A Comparison"

2.2 Sample Test Plan

Three commercially available wear/corrosion protection materials were selected for this study: austenitic 316 stainless steel, Stellite 6** which is Co-Cr based alloy, and IN-625* which is an austenitic Ni-Cr based alloy. Each material was deposited onto steel substrate by two methods: laser cladding and thermal spray, resulting in six different coating material conditions. The thickness of the deposits was varied from 8 to 40 mils (~ 0.2 to 1.0 mm) on flat sheet for open circuit potential (OCP) measurement and potentiodynamic testing. The sample description for OCP and Potentiodynamic testing is given in Table 1.

Table 1: Sample description of Open Circuit potential measurement and Potentiodynamic tests.

	Coating Material	Coating Process	Sample Identification
1	SS316	Laser Clad	LC 1316-14 mils (S1)
			LC 1316-30 mils (S2)
			LC 1316-30 mils (S3)
		Thermal Spray	816 S-10 mils (S1)
			816 S-11 mils (S2)
			816 S-11 mils (S3)
2	Stellite 6	Laser Clad	LC 1006-10 mils (S1)
			LC 1006-40 mils (S2)
			LC 1006-40 mils (S3)
		Thermal Spray	FWG 806 S-8 mils S (S1)
			FWG 806 S-10 mils (S2)
			FWG 806 S-12 mils (S3)
3	IN-625	Laser Clad	LC 1625-30 mils(S1)
			LC 1625-40 mils (S2)
			LC 1625-50 mils (S3)
		Thermal Spray	FWG 896 S-12 mils (S1)
			FWG 896 S-12 mils (S2)
			FWG 896 S-13 mils (S3)

"Corrosion Performance of Laser Clad Overlays and Thermal Spray Coatings: A Comparison"

A free standing cylindrical shell of solid coating roughly 80 mils (~ 2.0 mm) thick was used for gravimetric anodic corrosion testing. Briefly, three (3) samples per coating condition were utilized for OCP, potentiodynamic testing (2x thick + 1x thin), and three (3) samples per coating condition were utilized for gravimetric testing. One (1) sample per coating condition was utilized for characterization and micro hardness measurement. Table 2 has the sample description for Gravimetric testing.

Table 2: Sample description for Gravimetric test.

	Coating Material	Coating Process	Sample Identification
1	SS316	Laser Clad	S1 (~80 mils)
			S2 (~80 mils)
			S3 (~80 mils)
		Thermal Spray	S1 (~80 mils)
			S2 (~80 mils)
			S3 (~80 mils)
2	Stellite 6	Laser Clad	S1 (~80 mils)
			S2 (~80 mils)
			S3 (~80 mils)
		Thermal Spray	S1 (~80 mils)
			S2 (~80 mils)
			S3 (~80 mils)
3	IN-625	Laser Clad	S1 (~80 mils)
			S2 (~80 mils)
			S3 (~80 mils)
		Thermal Spray	S1 (~80 mils)
			S2 (~80 mils)
			S3 (~80 mils)

2.3 Open circuit potential measurement

OCP measurements were conducted in a corrosion cell configured as shown in Fig.2. The cell is made of Teflon with an interior volume of 6.8 fl oz (200 ml). The sample exposure orifice was sealed using rubber o-rings. The resulting exposed working electrode area was 0.121 in² (0.782 cm²).

The specimen was held in place using a clear epoxy back plate that was fastened to the cell. A copper strip was used to connect the sample to the potentiostat. Within the cell, a saturated calomel electrode was used as reference electrode, and the counter electrode was a coiled platinum wire positioned near the working electrode.

"Corrosion Performance of Laser Clad Overlays and Thermal Spray Coatings: A Comparison"

OCP measurements were conducted in 3.4% NaCl electrolyte, and held for 24 hours to allow for adequate stabilization. In one instance, for thermal sprayed Inconel, an additional test was conducted for a period of 168 hrs to establish a point of stabilization.

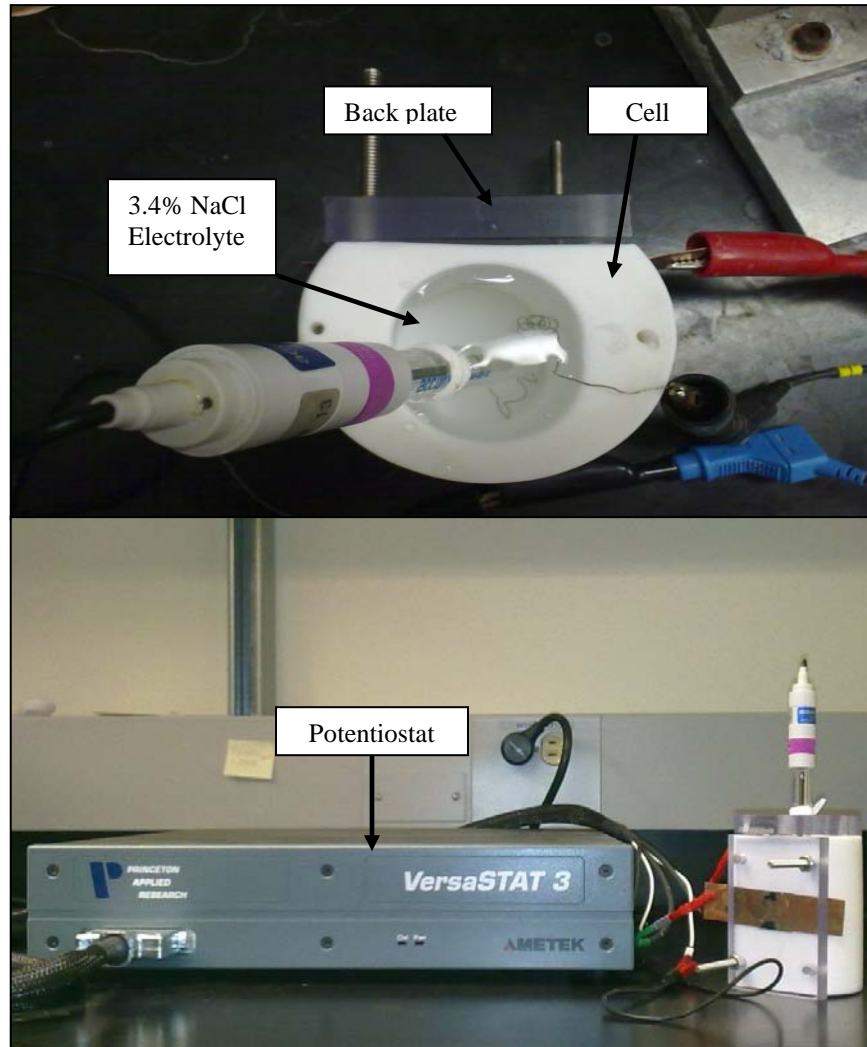


Fig. 2: Corrosion cell configuration

2.4 Potentiodynamic test

Potentiodynamic tests were conducted following OCP measurements under the same cell conditions to generate polarization curves (Tafel plots) and to determine the corrosion

"Corrosion Performance of Laser Clad Overlays and Thermal Spray Coatings: A Comparison"

current density for each coating material. The applied potential range was from -1 V to +2 V. Data was collected at a scan rate of 0.166 mV/s.

The following expression was used for calculating corrosion rate:

$$CPR = K \frac{A_w i_{corr}}{\rho n F} \quad \text{Eq.1 (Ref: Fontana, Corrosion Engineering)}$$

Where:

- CPR = Corrosion penetration rate in mils per year (mpy)
- K = 12,447 for corrosion rate unit in mpy
- A_w = Atomic weight of the corroding metal
- i_{corr} = Corrosion current density (μA/cm²)
- ρ = Density of the bulk metal (g/cm³)
- n = Number of electrons lost in the oxidation
- F = Faradays constant = 96,486 (C/mole)

$$\rho_{SS316} = 8.000 \text{ g/cm}^3, \text{ for Fe, } n=2$$

$$\rho_{Stellite 6} = 8.460 \text{ g/cm}^3, \text{ for Co, } n=2$$

$$\rho_{IN-625} = 8.440 \text{ g/cm}^3, \text{ for Fe, } n=2$$

Exposed area of sample (i.e. working electrode area) = 0.782 cm²

2.5 Gravimetric test:

The gravimetric corrosion test consisted of immersing the samples in 3.4% NaCl solution for 28 days. The samples were held at room temperature at 72°F (22°C) in glass jars (Fig 3) containing approximately 30 fl oz (900 ml) of solution sealed using an air tight lid. Periodic weight measurements were taken every 7 days to determine the corrosion rate by weight loss.

The test methodology was based on ASTM G31, Standard Practice for Laboratory Immersion Corrosion Testing of Metals.

The samples were cleaned before and after each weight measurement. More specifically, the cleaning sequence is as follows: each sample was wiped with soft Kimwipe tissue paper then immersed in acetone, ultrasonically cleaned for 15 min, wiped again with wet Kimwipe tissue paper, and finally blow dried using hot air.

"Corrosion Performance of Laser Clad Overlays and Thermal Spray Coatings: A Comparison"

The following expression was used for calculating corrosion rate:

$$CPR = \frac{KW}{\rho At} \quad \text{Eq. 2 (ref. ASTM G31)}$$

Where:

CPR = Corrosion penetration rate in mils per year (mpy)
K = 3.45×10^6 for corrosion rate unit in mpy
W = mass loss (g)
 ρ = Density of the bulk metal (g/cm^3)
A = Specimen area in (cm^2) = 47.5505 cm^2
t = Time interval in hrs ($24 \times 7 = 168$ hrs)

$\rho_{SS316} = 8.000 \text{ g}/\text{cm}^3$
 $\rho_{Stellite 6} = 8.460 \text{ g}/\text{cm}^3$
 $\rho_{IN-625} = 8.440 \text{ g}/\text{cm}^3$



Fig. 3: Gravimetric test continuous exposure setup

2.6 Characterization and Analysis

Various aspects of the coatings were studied to interpret the results of corrosion tests. Microstructural features were identified by using a field emission scanning electron microscope. Subject images were generated at magnifications ranging from 500X to 10,000X at an acceleration voltage of 20Kv using the secondary electron detector. Working distance was set at 10.7 m.

X-ray diffraction analysis was performed on a Bruker discover D8 2D x-ray diffractometer. Co $K\alpha$ radiation (wavelength 1.78897 \AA) was used for the stainless steel

"Corrosion Performance of Laser Clad Overlays and Thermal Spray Coatings: A Comparison"

and Inconel samples. Cu K alpha radiation of (wavelength 1.540598 Å) was used for the Stellite 6 samples.

Microhardness of the coatings was measured on cross sectioned flat samples using a Vickers micro-hardness indenter with a test force of 300 g, and indentation dwell time of 7 seconds. Five indentations were taken for each sample.

3. Results and Discussion

3.1 Open circuit potential measurement

As a general observation, OCP readings of the thermal sprayed coatings did not stabilize, even after 24 hours of exposure. Furthermore, the thermal sprayed coatings exhibited the common feature of an initial drop of OCP voltage, followed by a slow and very jagged increase over time. This can be explained by initial corrosion (oxidation), followed by a slow and inconsistent buildup of passive oxide layer. This hypothesis was tested by an additional experiment on thermal sprayed Inconel. In this case OCP readings were recorded for 168 hours, during which voltage values steadily climbed before appearing to reach a degree of relative constancy after 158 hours.

In comparison, OCP readings for laser clad coatings were less variable, and appeared to have reached near constant values at the end of 24 hours. The laser clad coatings did not exhibit the initial drop that was observed with thermal sprayed coatings. This might be explained by the fact that the laser clad coatings were less anodic (Fig.4), even from the start of OCP measurement; however, when the passivation layer formed, it was rapid and continuous thereby mitigating further corrosion. OCP potential measurement readings of IN-625 were a close match to wrought IN-625 [1].

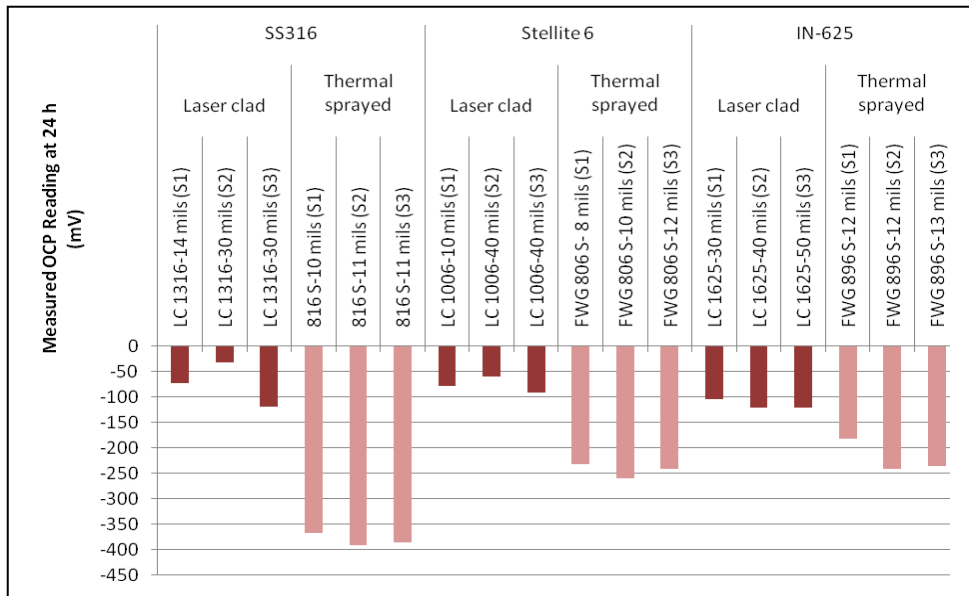


Fig. 4: OCP values measured at 24h of exposure

"Corrosion Performance of Laser Clad Overlays and Thermal Spray Coatings: A Comparison"

3.2 Potentiodynamic Test

The results of the potentiodynamic tests are presented in Table 3 in terms of corrosion potential E_{corr} , corrosion current I_{corr} , and corrosion penetration rate (CPR). CPR is calculated as a direct function of I_{corr}

The corrosion potential (E_{corr}) results indicate that laser clad coatings have higher corrosion potentials (i.e. less anodic) than thermal spray coatings. Among laser clad coatings, corrosion potential values are very similar. Among thermal sprayed coating, SS316 is most anodic, followed by Stellite 6 and IN-625.

Table 3: Potentiodynamic test results presented in terms of corrosion potential E_{corr} , corrosion current I_{corr} , and corrosion penetration rate (CPR)

		Sample ID	$E_{\text{corr}} \times 10^3$ (V)	$I_{\text{corr}} \times 10^{-09}$ (A)	CPR (mpy)
SS316	Laser clad	LC 1316-14 mils (S1)	-154.374	15.710	0.00905
		LC 1316-30 mils (S2)	-88.729*	2.308	0.00133
		LC 1316-30 mils (S3)	-186.841	8.522	0.00491
	Thermal sprayed	816 S-10 mils (S1)	-420.797	1402.000	0.80727
		816 S-11 mils (S2)	-440.200	1039.000	0.59825
		816 S-11 mils (S3)	-425.810	1252.000	0.72090
Stellite 6	Laser clad	LC 1006-10 mils (S1)	-185.110	4.920	0.00283
		LC 1006-40 mils (S2)	-170.480	4.229	0.00243
		LC 1006-40 mils (S3)	-190.260	7.172	0.00412
	Thermal sprayed	FWG 806 S- 8 mils (S1)	-18.682*	243.635	0.13999
		FWG 806 S-10 mils (S2)	-279.970	141.501	0.08130
		FWG 806 S-12 mils (S3)	-261.412	175.553	0.10087
IN-625	Laser clad	LC 1625-30 mils (S1)	-188.937	9.450	0.00542
		LC 1625-40 mils (S2)	-141.548	4.704	0.00270
		LC 1625-50 mils (S3)	-211.655	11.948	0.00685
	Thermal sprayed	FWG 896 S-12 mils (S1)	-43.000*	54.624	0.03134
		FWG 896 S-12 mils (S2)	-206.008	51.792	0.02971
		FWG 896 S-13 mils (S3)	-288.484	97.367	0.05586

"Corrosion Performance of Laser Clad Overlays and Thermal Spray Coatings: A Comparison"

Figure 5 represents the corrosion rate data using a log scale on the Y axis. This representation confirms that among laser clad coatings, corrosion rate values are very similar and extremely low corrosion rates. On the other hand, thermal sprayed coatings exhibited significantly greater corrosion rates, with SS316 having by far the highest corrosion rate, followed by Stellite 6 and IN-625. However, the corrosion resistance of thermal sprayed coatings can be improved by sealing the coating with polymers [4].

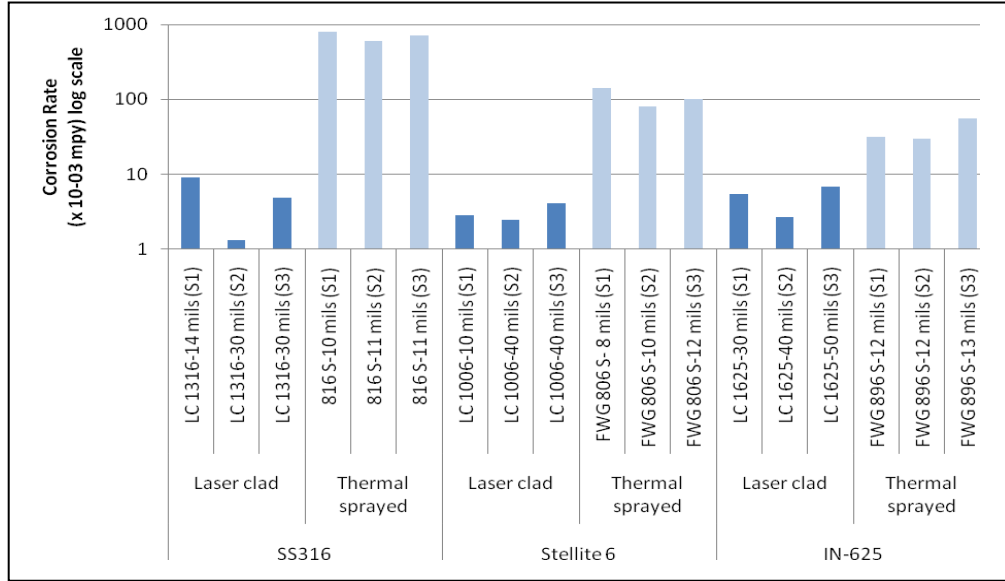


Fig. 5: Corrosion penetration rate (CPR) data represented in log scale

3.3 Gravimetric Test

The gravimetric test results are commented in terms of visible observations and gravimetric weight measurement data. No visible signs of corrosion were observed on any of the laser clad coatings. Thermal sprayed SS316 was clearly the most corroded coating. Bright red rust residues were visible in the solution and hard adherent red rust was visible on the specimen surface. Note that traces of surface corrosion remained on the thermal sprayed SS316 sample even after each cleaning operation. In the case of Stellite 6, a thin layer of corrosion product was observed, which was easily removed during each cleaning operation.

The gravimetric data shown in Table 4 and Fig 6 are consistent with the visual observations. Notably, the laser clad coatings sustained none or negligible weight loss. Among the thermal sprayed coatings, SS316 sustained by far the greatest weight loss, followed by Stellite 6 and IN-625. It is interesting to note that in the case of SS316, the greatest weight loss increments for all three samples occurred in the first week of

"Corrosion Performance of Laser Clad Overlays and Thermal Spray Coatings: A Comparison"

exposure. This was followed by the lowest weight loss increments during the second week of exposure.

Generally, it can be stated that the gravimetric test results were in agreement with the potentiodynamic test results.

Table 4: Gravimetric test data represented in terms of weight loss measured for each interval period, and total weight lost

		Weight reduction per 7 day period (g)					
		0- 7days	7- 14days	14-21days	21-28days	Total	
SS316	Laser clad	S1	0.0000	0.0000	0.0000	0.0000	0.0000
		S2	0.0000	0.0010	0.0000	0.0000	0.0010
		S3	0.0000	0.0010	0.0000	0.0000	0.0010
	Thermal sprayed	S1	0.0775	0.0081	0.0276	0.0308	0.1440
		S2	0.0564	0.0163	0.0307	0.0314	0.1348
		S3	0.0507	0.0134	0.0294	0.0313	0.1248
Stellite 6	Laser clad	S1	0.0000	0.0000	0.0000	0.0000	0.0000
		S2	0.0000	0.0000	0.0000	0.0000	0.0000
		S3	0.0000	0.0010	0.0000	0.0000	0.0010
	Thermal sprayed	S1	0.0086	0.0047	0.0114	0.0118	0.0365
		S2	0.0090	0.0096	0.0101	0.0103	0.0390
		S3	0.0099	0.0062	0.0111	0.0123	0.0395
IN-625	Laser clad	S1	0.0020	0.0000	0.0000	0.0000	0.0020
		S2	0.0000	0.0010	0.0000	0.0000	0.0010
		S3	0.0020	0.0000	0.0000	0.0000	0.0020
	Thermal sprayed	S1	0.0070	0.0087	0.0082	0.0102	0.0341
		S2	0.0075	0.0003	0.0057	0.0078	0.0213
		S3	0.0106	0.0047	0.0069	0.0079	0.0301

"Corrosion Performance of Laser Clad Overlays and Thermal Spray Coatings: A Comparison"

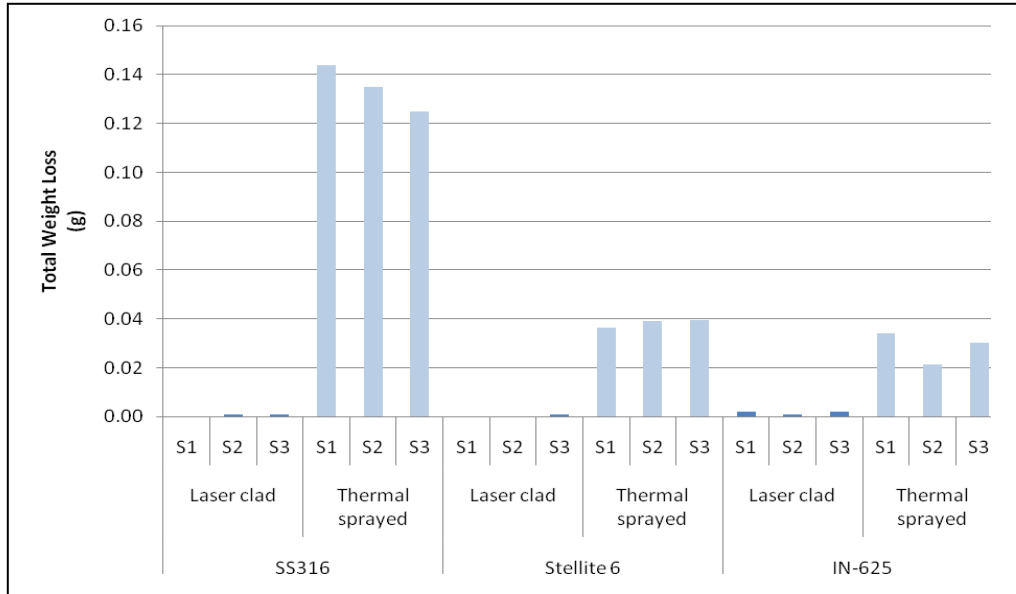


Fig. 6: Gravimetric data – total weight loss for each sample

3.4 SEM Characterization

SEM images of cross sections showing both coating and interface morphology indicated denser condition in the case of laser clad coatings as compared to the thermal sprayed coatings. Figure 5 shows the SEM image comparison of both laser clad and thermal spray samples. The laser clad coatings also appear both physically and metallurgically more homogeneous. Laser clad coatings contain negligible porosity and oxides. It is also evident that there is no significant grain growth in laser clad SS 316 and IN-625.

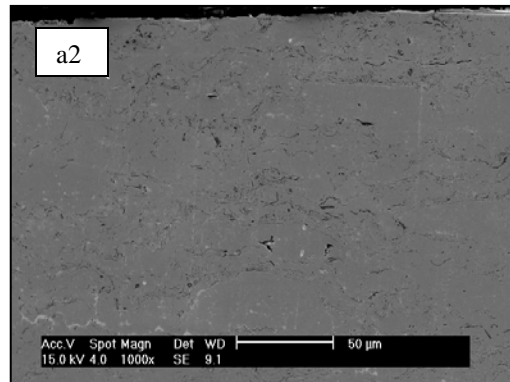
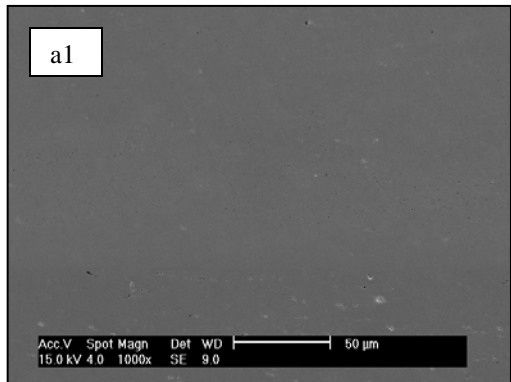
SEM images of Laser clad satellite 6 (Fig 7, b1) coating has dendritic microstructure containing carbides. This can be explained due to low energy input of the process, which has direct impact on scale of the dendrite formation. Since the laser clad process energy input is low, the solidification microstructure becomes finer and lower volume fractions of smaller interdendritic carbides are formed. This helps in improved wear and hardness properties of the coatings.

SEM images of thermal sprayed coatings show typical levels of porosity and oxidation which are higher as compared to laser clad coatings.

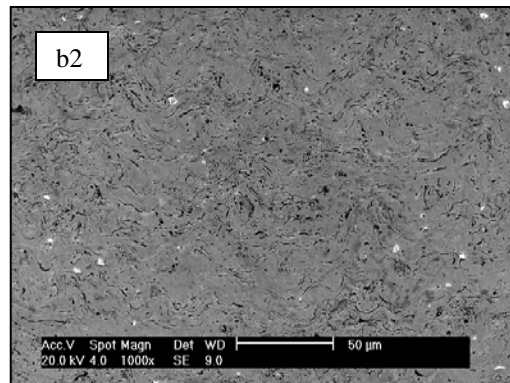
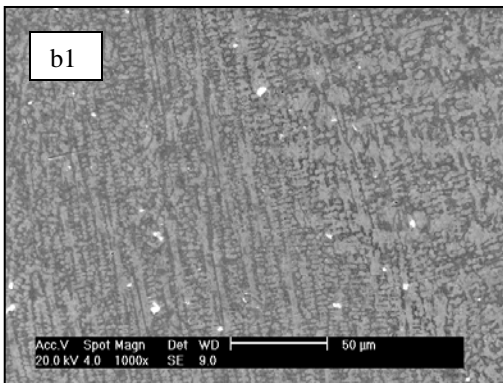
"Corrosion Performance of Laser Clad Overlays and Thermal Spray Coatings: A Comparison"

Laser Clad

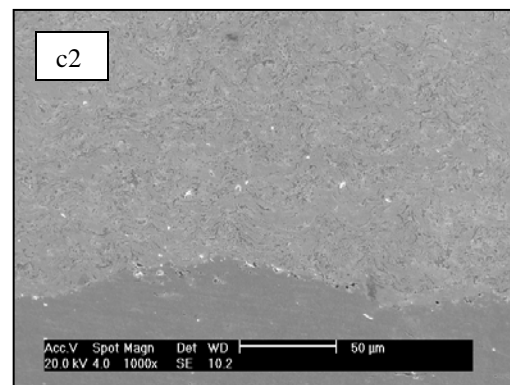
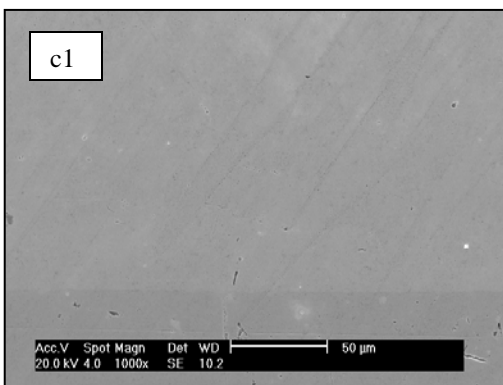
Thermal Spray



SS 316



Stellite 6



In-625

Fig. 7: SEM Images of Laser clad and Thermal spray Coating cross-sections

"Corrosion Performance of Laser Clad Overlays and Thermal Spray Coatings: A Comparison"

Laser Clad

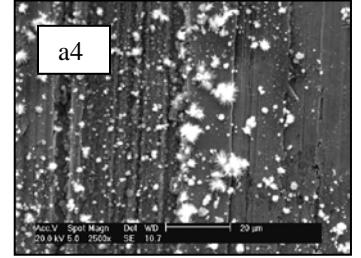
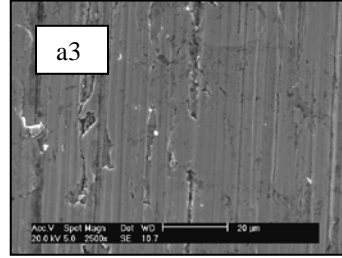
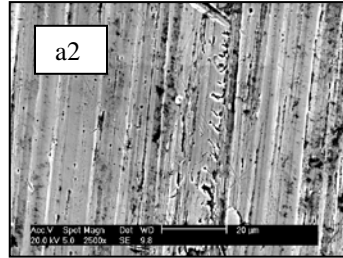
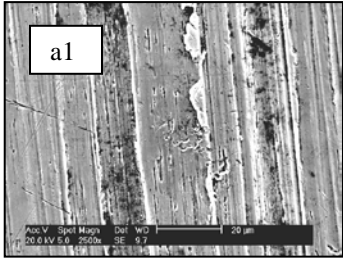
Thermal Spray

Unexposed

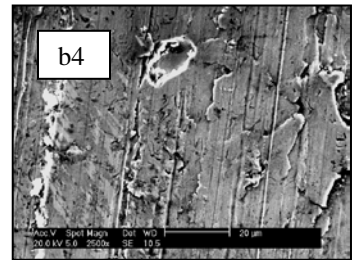
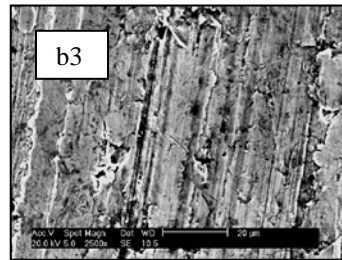
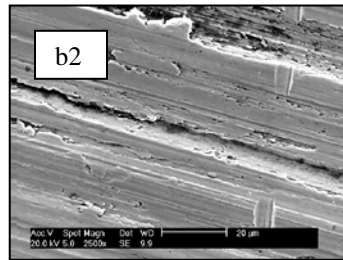
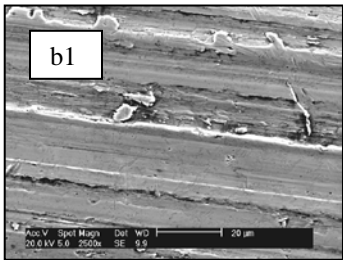
Exposed

Unexposed

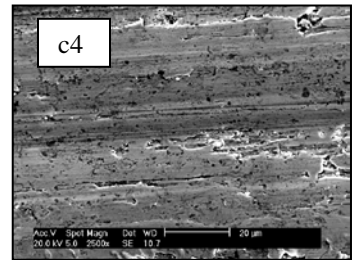
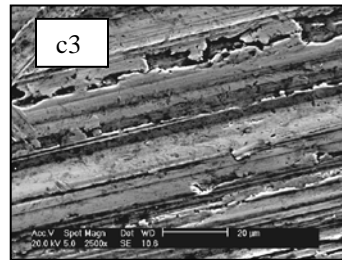
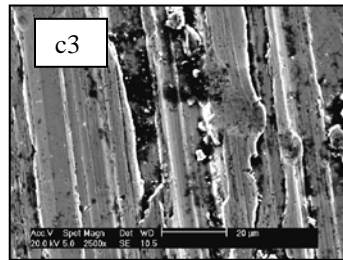
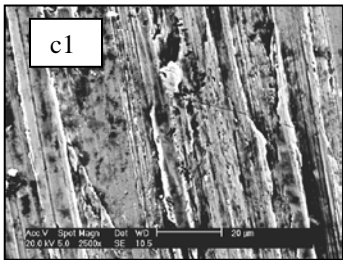
Exposed



SS 316



Stellite 6



In-625

Fig. 8: SEM images of Laser clad and Thermal spray Coatings surface morphology

SEM images were taken at surface of flat samples (Fig 8). Surface images included unexposed areas as well as areas corroded during potentiodynamic testing.

When comparing the appearance of exposed surfaces to non-exposed surfaces, the laser clad coatings appeared unchanged. In the case of the thermal spray coatings, SS316 exhibited by far the greatest amount of corrosion products on the exposed surface (Fig 8, a4). IN-625 (Fig 8, c3) exhibited evidence of pitting on the exposed surface, whereas Stellite 6 appeared largely unchanged. SEM observations are consistent with the results of the corrosion tests described previously.

"Corrosion Performance of Laser Clad Overlays and Thermal Spray Coatings: A Comparison"

3.5 XRD Characterization

Stellite 6 and IN-625 were composed of single phase materials from XRD results. SS316 was composed of two phases, ferrite and austenite, in proportions given in Table 5.

Table 5: Proportions of ferrite and austenite in laser clad versus thermal sprayed SS316

SS316 Laser clad 30mils		
03-065-4899	9.60%	Fe ferrite
03-065-4150	90.40%	Fe austenite
SS316 Thermal Sprayed 10 mils		
03-065-4150	35.10%	Fe ferrite
03-065-4899	64.90%	Fe austenite

3.6 Microhardness

Microhardness values showed that for each material, thermal spraying results in a harder deposited coating as compared to laser cladding. It is observed that thermal spray coatings are significantly harder than laser clad coatings, which can be explained due to higher oxide content. Among the different materials, irrespective of the method of deposition, Stellite 6 is the hardest coating material, followed by IN-625 and SS316 (Fig 9).

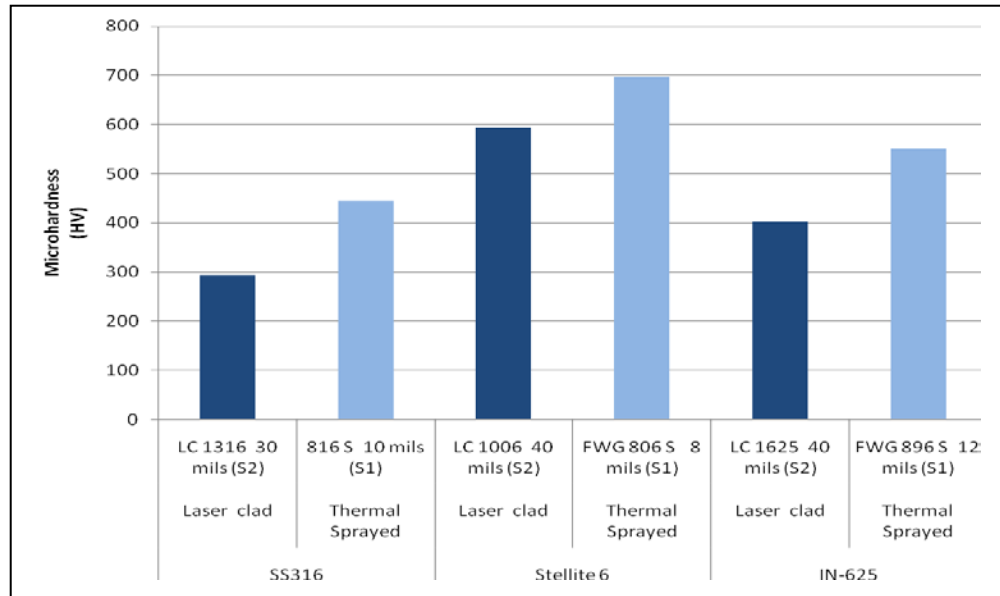


Fig. 9: Average measured microhardness values (HV) for each coating condition

"Corrosion Performance of Laser Clad Overlays and Thermal Spray Coatings: A Comparison"

4. Conclusions

This research addresses the comparison study of corrosion resistance characteristics of laser clad and thermal spray coatings. The following are the conclusions drawn:

1. Laser clad coatings display superior corrosion resistance when compared to HVOF thermal spray coatings.
2. Microstructure analysis of the SEM images shows that the laser clad coatings contain negligible porosity when compared to thermal spray coatings. This could explain the superior corrosion resistance of laser clad overlays.
3. Surface morphology analysis of the exposed and unexposed samples during potentiodynamic testing proves that the laser clad coatings remain unchanged whereas thermal spray coatings exhibited significant surface corrosion.
4. It is evident from the XRD results that both laser clad and thermal spray coatings of SS316 contain both ferrite and austenite phases. The higher percentage of ferrite phase in thermal sprayed coating supports the higher corrosion rate obtained and the SEM images of exposed surfaces during potentiodynamic test (Table 5).
5. Thermal spray coatings proved to be harder when compared to laser clad coatings. This can be explained by the presence of more oxides in thermal spray coatings.

5. References

- [1] P. Vuristo, J. Vihinen, Maintenance Research, (2002)
- [2] S. Simard, B. Arsenault, National Thermal Conf. Vol.1 (2003), Materials Park, Ohio.
- [3] D. Chidambaram, C.R. Clayton, M.R. Dorfman, Surface Coatings & Tech 192 (2005) 278-283.
- [4] D. Chidambaram, C.R. Clayton, M.R. Dorfman, Surface Coatings & Tech 176 (2004) 307-317.
- [5] P. Siltonen, T. Konos, P. O. Kettunen, National Thermal Conf. (1994), Boston, Massachusetts.
- [6] J. Kawakita, T. Fukushima, S. Kuroda, T. Kodama, Corrosion Science 44 (2002) 2651-2581.
- [7] M. Magnani, P.H. Suegama, A. Andre, C. Recco, J. M. Guilemany, C. S. Fugivara, A.V. Benedetti, Materials Research, 10 (2007) 377-385.
- [8] M. Magnani, P.H. Suegama, N. Espallargas, S. Dosta, C.S. Fugivara, J.M. Guilemany, A.V. Benedetti, Surface & Coatings Tech, 202 (2008) 4746-4757.
- [9] J.M. Guilemany, J. Fernandez, J. Delgado, A.V. Benedetti, F. Climent, Surface & Coatings Tech, 153 (2002) 107-113.
- [10] P.H. Suegama, C.S. Fugivara, A.V. Benedetti, J. Fernandez, J. Delgado, J.M. Guilemany, Corrosion Science, 47 (2005) 605-620.